Figure S1

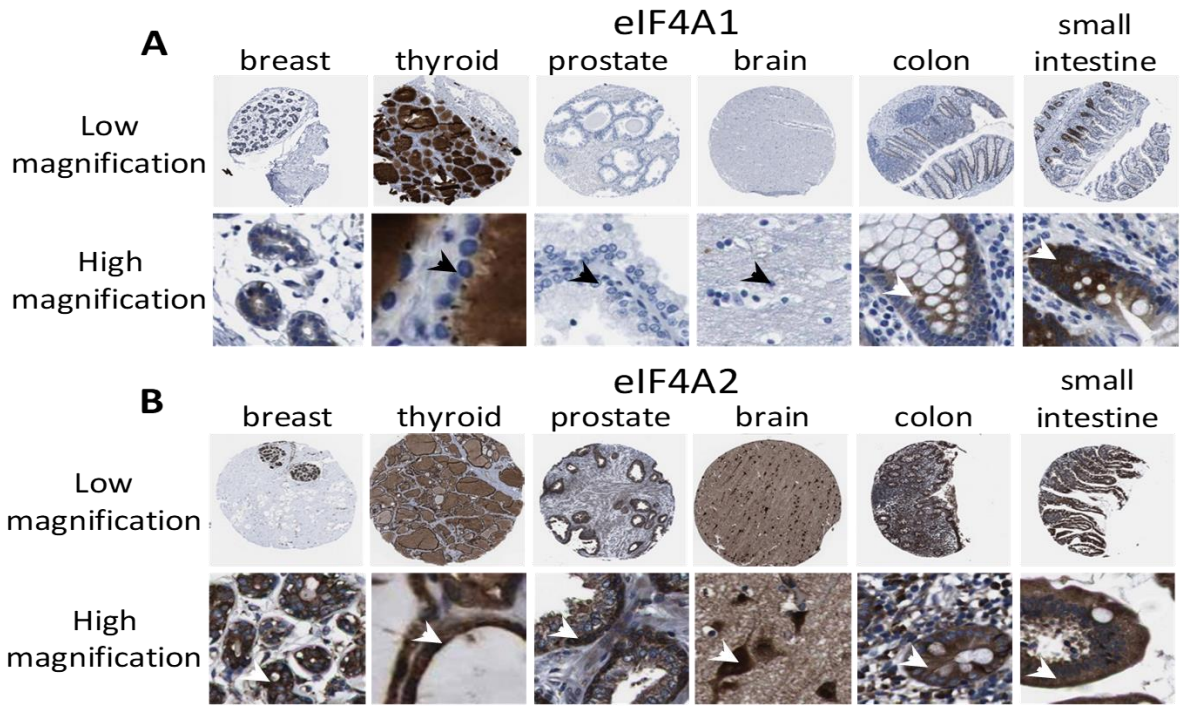

Fig. S1 (A-B) eIF4A paralogues expression across tissues. eIF4A1 is negative in most mature epithelia (arrows in thyroid and prostate) and mesenchymal tissues including brain. There is however a strong expression in proliferative crypts of colon and small intestine. eIF4A2 expression is however, highly differentiated cells (white arrows pointing to cortical neurons in brain) and secretory epithelia (white arrows in breast ducts and secretory villi from the small intestine). Core images from the Human Protein Atlas.

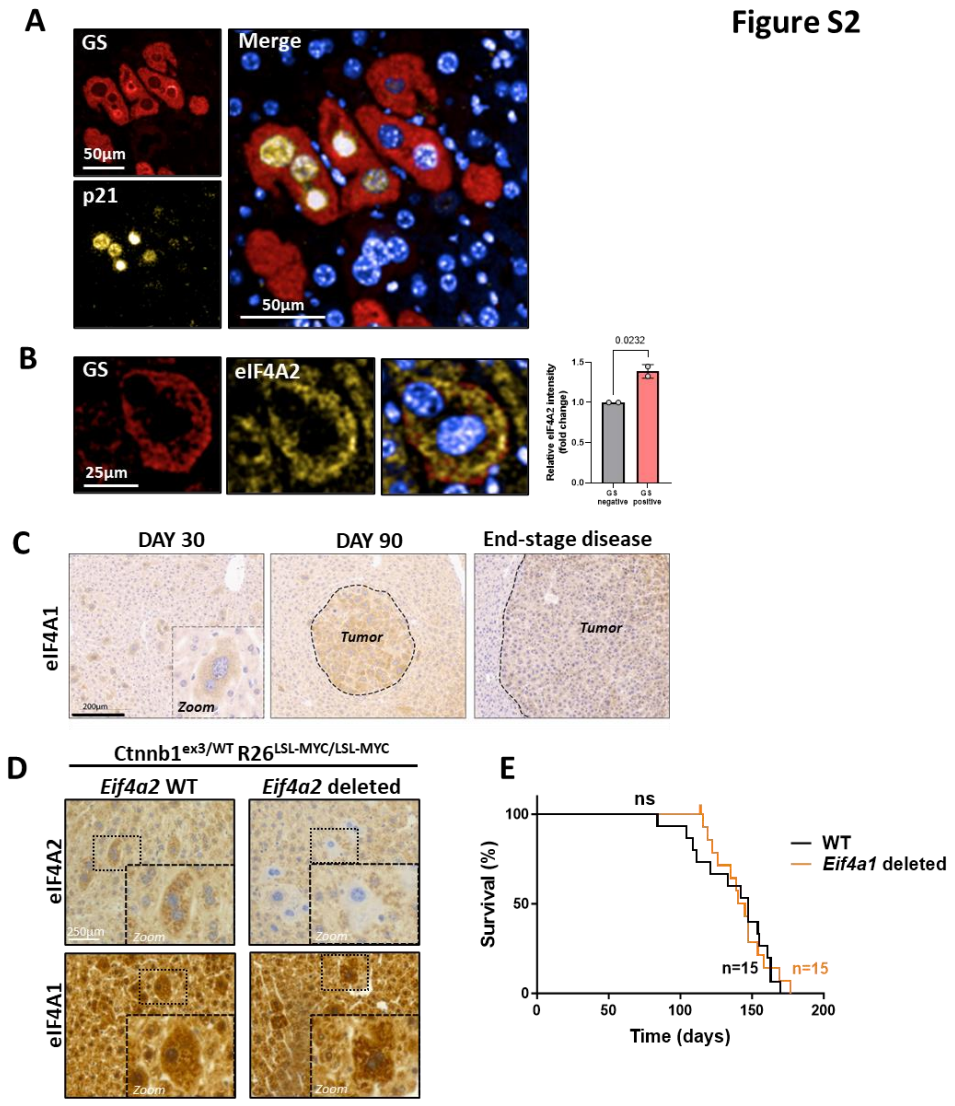

Fig. S2 (**A-B**) **Immunofluorescence visualization of p21 and eIF4A2 in HCC initiating cells.** *Ctnnb1*$^{ex3/WT}$; *Rosa26*$^{LSL-MYC/LSL-MYC}$ mice were injected (i.v.) with AAV-TBG-Cre (6.4 X 10^8 genome copies (GC) per mouse; a titre sufficient to evoke recombination in ≈5% hepatocytes). Mice were sacrificed 30 days following this and glutamine synthetase (GS; an indicator of activated β-catenin signaling) was visualized with respect to p21 (A) or eIF4A2 (B) in zone 2 of the liver by immunofluorescence. The intensity of staining for eIF4A2 in GS-positive and GS-negative hepatocytes was determined using high-content analysis - each data point in (B) represents quantification from an individual mouse, mean±SEM, statistical test was student's unpaired t-test.

(C) Expression of eIF4A1 during HCC progression. *Ctnnb1*$^{ex3/WT}$; *Rosa26*$^{LSL-MYC/LSL-MYC}$ mice were injected with AAV-TBG-Cre as for A and sacrificed 30 or 90 days following this or were left till tumour endpoint (end-stage disease) was reached. eIF4A1 was visualized using immunohistochemistry.

(D) Knockout of *Eif4a2* in HCC tumor initiating cells. *Ctnnb1*$^{ex3/WT}$; *Rosa26*$^{LSL-MYC/LSLMYC}$ mice that were either *Eif4a2*$^{WT/WT}$ or *Eif4a2*$^{fl/fl}$ were injected (i.v.) with AAV-TBG-Cre (6.4 X 10^8 GC per mouse). Mice were sacrificed 30 days following this and eIF4A1 and eIF4A2 were visualized in zone 2 of the liver by immunohistochemistry.

(E) Hepatocyte-specific knockout of *Eif4a1*does not influence initiation or progression of HCC. *Ctnnb1*$^{ex3/WT}$; *Rosa26*$^{LSL-MYC/LSL-MYC}$ mice that were either *Eif4a1/Eif4a2*$^{WT/WT}$ or *Eif4a1*$^{fl/fl}$ were injected (i.v.) with AAV-TBG-Cre (6.4 X 10^8 GC per mouse). Mice were sacrificed at tumour endpoint and the time (in days) to endpoint was recorded. Statistical test, Log rank (Mantel-Cox).

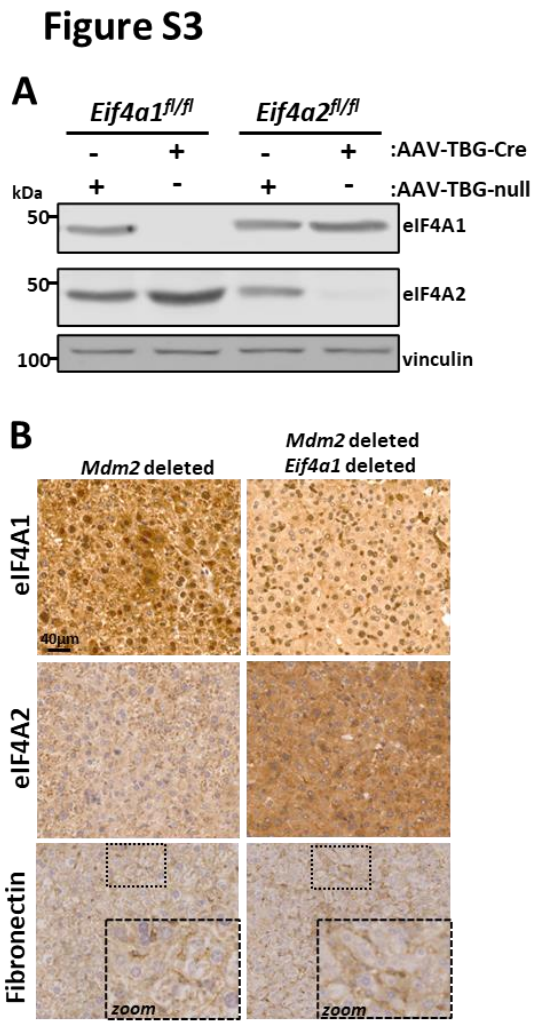

Fig. S3. Roles and expression of eIF4As and fibronectin in liver senescence

(A) Hepatocyte-specific deletion of eIF4A paralogues. Mice bearing floxed alleles of *Eif4a1* (*Eif4a1*$^{fl/fl}$) or *Eif4a2* (*Eif4a2*$^{fl/fl}$) were injected with AAV-TBG-Cre (2 X 10^{11} GC per mouse; a titre sufficient to evoke recombination in >90% hepatocytes) and sacrificed 30 days later. Livers were removed and homogenized. Levels of eIF4A1, eIF4A2 in liver homogenates were determined by Western blotting with vinculin as loading control.

(B) eIF4A1 deletion does not oppose FN deposition following induction of hepatocyte senescence. Mice bearing floxed alleles of *Mdm2* (*Mdm2*$^{fl/fl}$) that were either *Eif4a1* WT (*Eif4a1*$^{WT/WT}$) or *Eif4a1* floxed (*Eif4a1*$^{fl/fl}$) were injected with AAV-TBG-Cre as for (**A**). 4 days following this, livers were fixed as eIF4A1, eIF4A2 and fibronectin visualized using immunohistochemistry.

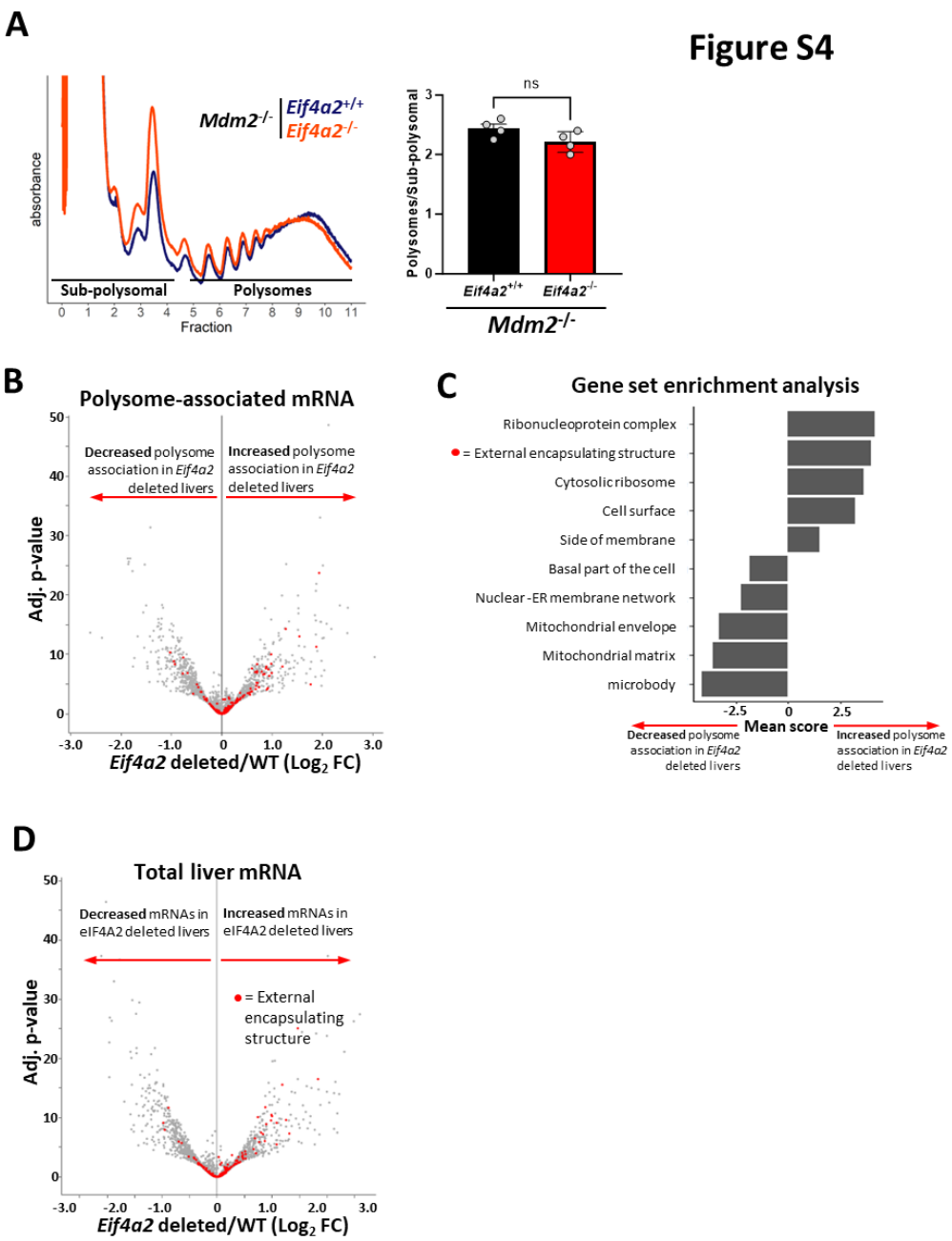

Fig. S4. Polysome profiling of wild-type and *Eif4a2* knockout livers

Mice bearing floxed alleles of *Mdm2* (*Mdm2*$^{fl/fl}$) that were either *Eif4a2* WT (*Eif4a2*$^{WT/WT}$) or *Eif4a2* floxed (*Eif4a2*$^{fl/fl}$) were injected with AAV-TBG-Cre (2 X 10^{11} GC per mouse). 4 days following this, livers were homogenized in the presence of cycloheximide and polysomes and sub-polysomes were resolved using sucrose-density gradient centrifugation. The ratio of polysome to sub-polysomes was calculated and is displayed in (**A**). Total (**D**) and polysome-associated (**B, C**) mRNAs were determined by RNAseq. GSEA was performed using the GO term 'cellular component' as a reference, and the output from this was ranked according to polysome-associated log2FCs. Redundant terms were collapsed using rrvgo. Terms enriched in genes translationally upregulated following *Eif4a2* deletion have positive scores (**C**). This analysis indicates that mRNAs encoding genes from the external encapsulating structure are enriched in polysomes from *Eif4a2*-deleted livers (**C**) and these are highlighted by red dots in the volcano plots in (**B,D**).

Figure S5

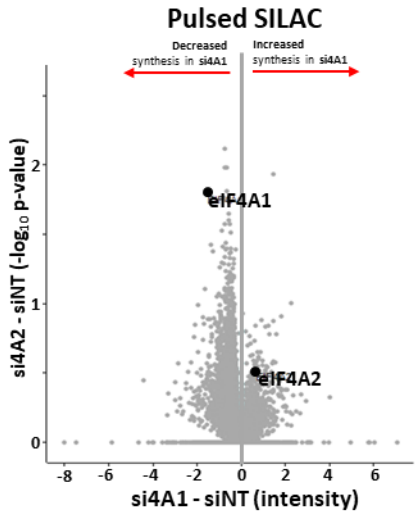

Fig. S5. Pulsed-SILAC indicates that eIF4A1 knockdown reduces protein synthesis rates. Fibroblasts were transfected with either non-targeting (siNT) oligonucleotides or those targeting eIF4A1 (si4A1) and were incubated with 'heavy' SILAC amino acids (Arg10 & Lys8) for 16h (pulsed-SILAC). Lysates were digested with trypsin and tryptic peptides analysed using mass spectrometry to reveal the influence of eIF4A1 knockdown on the newly synthesized proteome. Data are plotted as differences in intensity (abscissa) and statistical significance (ordinate) between eIF4A1 knockdown and control (si4A1 – siNT).

Figure S6

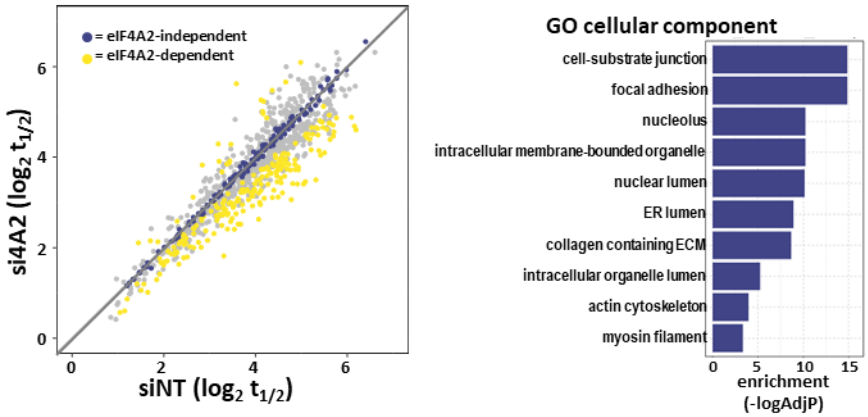

Fig. S6. GO terms of proteins whose turnover is increased by eIF4A2 knockdown. Control and eIF4A2 knockdown fibroblasts were incubated with 'heavy' SILAC amino acids for the times indicated in Fig. 5A, and tryptic peptides were tandem mass-tagged (TMT) and analysed using mass spectrometry-based proteomics. Turnover rates were derived from the proteomic data and proteins with significantly different $t_{1/2}$s are denoted using yellow dots (eIF4A2-dependent; left panel). The gene ontology (GO) terms for proteins with significantly different $t_{1/2}$ are ranked in the right panel.